J Appl Electrochem (2008) 38:1519–1526
DOI 10.1007/s10800-008-9596-1

ORIGINAL PAPER

Electrochemical gold deposition from sulfite solution: application for subsequent polyaniline layer formation

Gintaras Baltrūnas · Aušra Valiūnienė · Justas Vienožinskis · Ernestas Gaidamauskas · Teofilis Jankauskas · Žana Margarian

Received: 10 November 2006 / Accepted: 14 May 2008 / Published online: 27 May 2008

Abstract Electrochemical gold deposition from sulfite solutions was studied by means of voltammetry, EIS and EQCM. A gold film electrode was used for polyaniline layer formation by electrochemical oxidation of aniline. The standard electrochemical reduction potential of the reaction $[Au(SO_3)_2]^{3-} + e^- = Au + 2\ SO_3^{2-}$ was determined, and is equal to 0.116 V (vs. NHE). Both solution stirring and temperature increase accelerate the electrochemical reduction of gold, when the electrode potential is below −0.55 V. When the potential is above −0.55 V the electrochemical reduction proceeds via passive layer formation. Our study suggests that the passive layer consists of chemically adsorbed sulfite ions and sulfur. The gold film deposited from sulfite solution is a high quality substrate suitable for conducting polymer layer formation. This technique, where a polymer layer electrode is prepared by thin gold film deposition onto a metal surface and by subsequent polymer layer formation, can be applied in sensor research and technology.

Keywords Adsorption · Electrochemical impedance spectroscopy · Gold · Passive layer · Sulfite · Sulfur · Microbalance

1 Introduction

Electrochemically conducting polymer layers are widely used in technology as functional components for electrochemical power sources, accumulators, and bio-sensors [1, 2]. They are readily obtained by electrochemical monomer oxidation on a noble metal surface [3]. However, the high cost and mechanical incompatibility may preclude the use of a bulk metal substrate in some cases. A metal film electrochemically deposited on a conducting substrate (for example, steel, titanium) offers an effective way to solve these problems.

Although electrochemical gold reduction from cyanide containing solution remains the popular gold plating process [4], cyanide toxicity and incompatibility limits its use in newly developing application areas. Gold plating from a sulfite complex is one plausible alternative to cyanide suggested by Smith [5]. The high-quality gold film deposition from a solution with a trace amount of As(III) was reported later [6], and gold film with superior properties was described. Recently a number of processes based on gold reduction from sulfite were formulated to obtain gold films suitable for X-ray lithography and microtechnical devices [7–10].

Previously reported gold(I) sulfite complex $[Au(SO_3)_2]^{3-}$ stability constants vary from 10^{28} [11] to 10^{12} [12]. Shirai et al. [13] proposed the following mechanism for electrochemical gold reduction: the step-wise complex dissociation in the first two steps: (1) $[Au(SO_3)_2]^{3-} \rightarrow [Au(SO_3)]^- + SO_3^{2-}$, (2) $[Au(SO_3)]^- \rightarrow Au^+ + SO_3^{2-}$, and a subsequent charge transfer (3) $Au^+ + e^- \rightarrow Au$. Above ambient temperature the electroless deposition mechanism was proposed [14, 15], and instead of the charge transfer step in the mechanism above, gold(I) disproportionation was suggested: $3Au^+ \rightarrow 2Au + Au^{3+}$. Chronoammetry and EIS studies [16] showed that when electrode potential is below −0.5 V, the reaction rate is affected by the surface passivation caused by the slow sulfite ion adsorption and desorption and by the chemical compound formation on the metal surface.

G. Baltrūnas (✉) · A. Valiūnienė · J. Vienožinskis · E. Gaidamauskas · T. Jankauskas · Ž. Margarian
Faculty of Chemistry, Vilnius University, Naugarduko 24, 03225 Vilnius, Lithuania
e-mail: gintaras.baltrunas@chf.vu.lt

A radioactive indicator study [17] of sulfite ion adsorption on gold has shown that in 2×10^{-4} M neutral sulfite solutions adsorption of SO_3^{2-}reaches the maximum value of 3×10^{-10} mol cm^{-2} when potential is 1.2 V, i.e. where the SO_3^{2-} is rapidly oxidized. At more negative potentials the number of adsorbed SO_3^{2-} species remains high; for instance, at $E = 0.0$ V it exceeds 10^{-10} mol cm^{-2}. The ^{35}S surface concentration dynamics suggests that the SO_3^{2-} adsorption is very slow-step with an equilibration time above 10^3 s. Formation of a chemical compound on the gold surface was also proposed [17]. In-situ Raman spectra acquired at −0.8 V exhibit the SO_3^{2-} signal, and sulfite release after the electrochemical reaction was suggested. The S–S signal observed at −0.3 V shows a sulfur layer formation on the electrode surface [18]. Upon increase in Au(I) complex concentration from 0.05 to 0.5 M the sulfur layer stability also increases. At negative potentials the sulfur reduction to HS^- was expected, however, no S–H signal was detected. The adsorbed SO_3^{2-} anion is attached to the surface either via an oxygen or via a sulfur depending on the electrode potential, and the transition from the oxygen-attached to the sulfur attached anion takes place at −0.5 V during the negative potential scan. Elemental sulfur formation and its incorporation into gold films was also reported in a EQCM study [19], however, the sulfur layer formation cannot be attributed unambiguously to the sulfite, since a sulfite and thiosulfite solution was used in this study.

A polyaniline layer is readily prepared on gold or platinum electrodes by anodization in acidic aniline solutions. Polyaniline layer protonation (deprotonation) and oxidation (reduction) is completely reversible, since neither reactions affect the inner layer structure, and once formed on the surface, the polymer layer remains stable. Polyaniline layers exhibit acceptable conductivity only in acidic solutions (pH below 3), and in a narrow potential window from 0.3 to 0.7 V [3].

The double layer of the polycrystalline electrode in solution is usually simulated as the constant phase element (CPE) with impedance given by Eq. 1 [20]. Factor A corresponds to the average double layer capacitance and the exponent n shows the impedance phase shift. When the electrode surface is homogeneous, n is unity, and Eq. 1 transforms into the simple capacitor impedance Eq. 2

$$Z_{CPE} = A^{-1}(j\omega)^{-n} \quad (1)$$

$$Z_{CPE} = (C_D j\omega)^{-1}. \quad (2)$$

Deviation of the exponent n from unity is usually small even for a rough metal surface and is within the 0.9–1 range. However, the n deviation may increase drastically when the metal surface is covered with a low conductivity layer, for example, the oxide layer [20]. One can expect that formation of sulfur and especially polymer layers on the electrode surface should significantly affect the n values. Of course, formation of polymer layers will also change the equivalent circuit.

In this study we focused on gold deposition onto a metal surface from sulfite solution as a promising way of preparing a substrate suitable for subsequent conducting polymer layer synthesis. The influence of sulfite ion adsorption on the gold(I) sulfite reduction kinetics and deposition parameters, important from the practical point of view, were also explored.

2 Experimental

Solutions were prepared from an Au(I) sulfite complex stock solution (Imabrite 24, Schlotter, Germany), and "p.a." grade Na_2SO_3, Na_2SO_4, and $HClO_4$ compounds. Aniline was purified by distillation in a vacuum. Doubly distilled water was used throughout. The gold amalgam electrode was prepared by galvanostatic mercury film deposition (2 mg) on a Pt rod electrode (surface area 0.16 cm^2) from a mercury nitrate solution, and a subsequent gold deposition (0.01 mg) from sulfite solution. The gold amalgam electrode was kept in distilled water overnight before use. The Gibbs energy difference was evaluated from the potential difference between the bulk gold and the amalgam electrode in a solution containing 0.05 M of $K[Au(CN)_2]$ and 0.01 M of KCN. Pt and Ti rod electrodes were electrochemically plated with gold from a sulfite solution. The solution composition was as follows (in M): Au(I)—0.05, Na_2SO_3—0.5, As_2O_3—3×10^{-5}, and the pH was 9.5.

Voltammetry and EIS experiments were performed using a μAUTOLAB (Type III) electrochemical modular system with a standard three-electrode electrochemical cell. The working electrode was a gold plated (thickness 1 μm) Pt rod (0.16 cm^2). The reference electrode was an Ag/AgCl (3 M KCl) electrode, and the counter electrode was a Pt cylinder (20 cm^2). All electrode potentials shown in this work (E_H) are converted to the NHE scale. For the impedance measurements an AC-amplitude of 3 mV was used. In the present investigation a sum of 48 sine waves distributed over 4.8 decades (0.05–4,000 Hz) in logarithmic scale was used. The parasitic capacitance of the electrochemical circuit reached approximately 1,200 pF. In order to decrease distortion relating to the parasitic capacitance, the upper frequency was limited to 4,000 Hz.

AT cut 5 MHz quartz crystals (diameter of 15 mm and thickness of 0.3 mm) sputtered with a disk-shaped gold layer (diameter of 6 mm and thickness of 100 nm) were used for the electrochemical quartz crystal microbalance (EQCM) study. The piezoelectrically active surface area was 0.21 cm^2. All resonators were calibrated by galvanostatic

silver deposition at 50 μA from silver nitrate solution (M): $AgNO_3$—0.015 and KNO_3—0.1. The sensitivity constant was 6.06 ng Hz^{-1}.

3 Results and discussion

3.1 Electrochemical reduction of gold from gold(I) sulfite complexes

Attempts to measure the equilibrium potential directly on gold electrode were not successful. Presumably, the exchange current density is too low, and as a result, the electrode potential is unstable and sensitive even to a small electrostatic charge. Reliable equilibrium potentials were obtained with a gold amalgam electrode. The values of gold amalgam electrode potentials were obtained as a function of the [Au(I)] when $[SO_3^{2-}] = 0.5$ M as well as of the sulfite concentration when [Au(I)] = 0.05 M (Fig. 1). The potentiometric curve analysis revealed the predominance of the $[Au(SO_3)_2]^{3-}$ complex ions in the bulk solution. The slope of the linear fit to the experimental data points provided a standard electrochemical potential for the couple $Au/[Au(SO_3)_2]^{3-}$ equal to 0.116 V. This value corresponds to the logarithm of the $[Au(SO_3)_2]^{3-}$ stability constant 27.4, which is similar to the previously reported result [11].

Our previous rotating disk electrode study [21] suggests that the electrochemical reduction of gold sulfite complexes is limited mostly by diffusion, except for a small cathodic polarization region below −0.6 V, where the limiting current density does not depend on the rotation speed. The voltammetric curves recorded in gold sulfite solutions are sensitive to the surface active species (for instance, Se^{2-}) and electrode cleanliness. Similar behavior is observed for electrochemical silver reduction from cyanide solutions, where the reaction rate is limited by surface passivation [22].

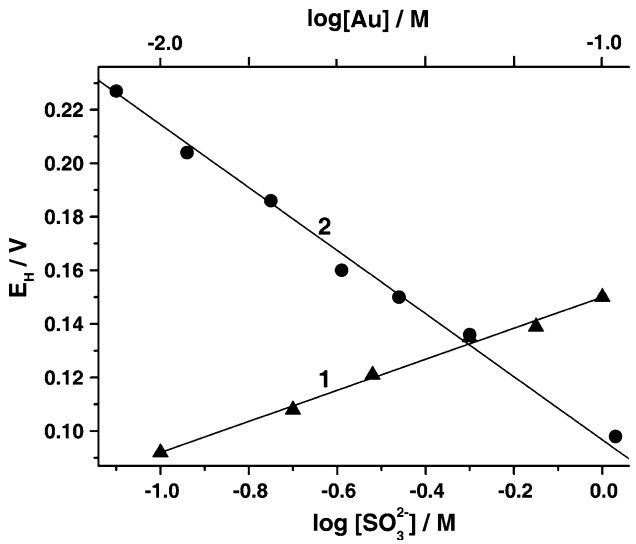

Fig. 1 Gold amalgam Au(Hg) equilibrium potential as a function of gold(I) sulfite (1) and free sulfite (2) concentration

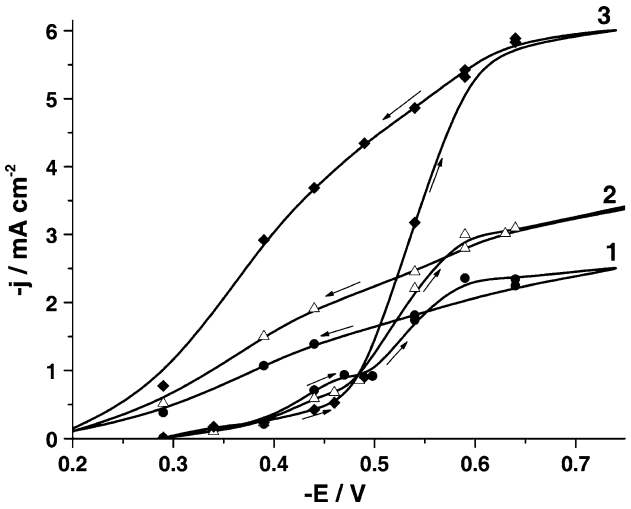

Fig. 2 The voltammetric curves of electrochemical gold(I) sulfite complex reduction. Solution composition is as follows (M): Au(I)—0.05, Na_2SO_3—0.5, and As_2O_3—3×10^{-5}. Solution pH is 9.5. Potential scan rate is 5 mV s^{-1}. Solution temperature (°C): 1—30, 2—45, and 3—65

A low limiting current density is the major problem in practical gold plating from sulfite solutions. This can be solved by increasing the plating temperature. Although higher temperature usually increases the limiting current density, its application may not be suitable for practical purposes. Therefore, we examined the temperature effect on gold deposition from sulfite solutions in more detail. For this purpose cyclic voltammograms were acquired at various temperatures from 23 to 65 °C. Figure 2 shows three typical curves.

The current density increases with temperature when cathodic polarization is higher than −0.6 V, and the current density as a function of potential, does not depend on scan direction. In a small polarization zone ("passive" zone) significant hysteresis is observed on the negative and positive potential scan direction.

At higher temperatures the hysteresis increases, and moreover, in the potential region −0.4 to −0.5 V the current density decreases with temperature. This effect is not observed during the reverse scan. Cycling of electrode potential decreases the hysteresis, and the positive scan curve shifts towards the negative scan curve, albeit not completely.

It was determined that the dependence of limiting current density on temperature in coordinates log j vs. $1/T$ is linear at any electrode potential. Thus, we have used $d(\log j)/d(1/T)$ as the thermal coefficient of the rate of the process. The temperature coefficient $[d(\log j)/d(1/T)]_E$ multiplied by 2.303R

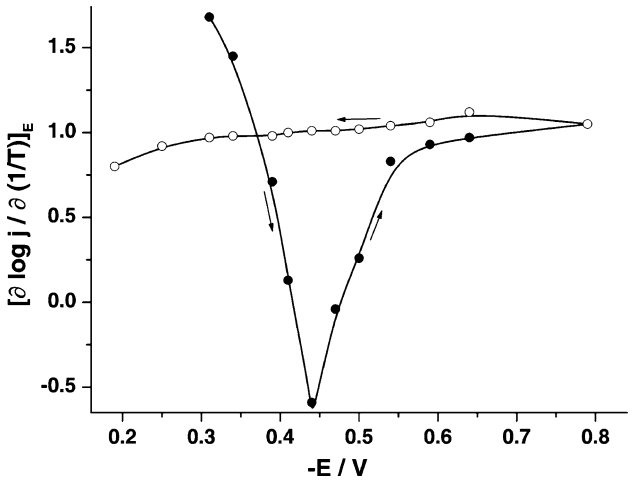

Fig. 3 The reaction temperature coefficient of gold(I) reduction from sulfite solution plot versus gold electrode potential. Potential scan rate is 5 mV s^{-1}. Arrows show the potential scan direction

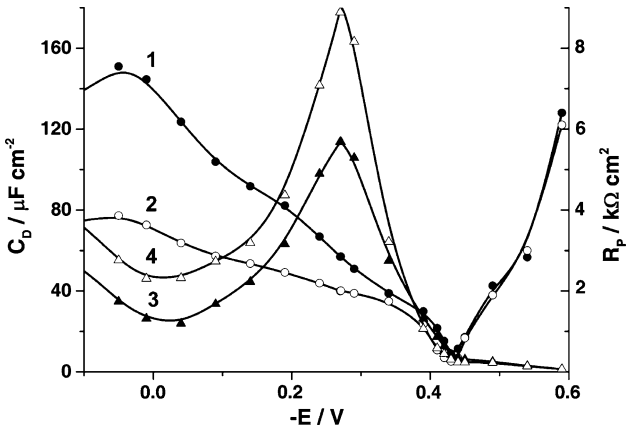

Fig. 4 Parallel capacitance (1, 2) and polarization resistance (3, 4) are shown as functions of gold electrode potential. Potential scan rate is 0.5 mV s^{-1} (1, 3) and 2 mV s^{-1} (2, 4). The AC frequency is 3 Hz. Solution composition the same as in Fig. 2

yields the "effective activation energy E_A of an electrochemical reaction" [23]. However, when reaction is limited by diffusion or passivation the meaning of E_A is complex and not always obvious. The temperature coefficient rapidly decreases during the cathodic scan from 1.68 ($E_A = 32$ kJ mol^{-1}) at −0.31 V to −0.59 at −0.44 V, and passing through the minimum reaches a constant value close to 1 ($E_A = 20$ kJ mol^{-1}) at −0.55 V. In the positive potential scan the temperature coefficient remains constant up to −0.19 V. These effects are due to compact passive layer formation, which inhibit electrochemical reduction of gold sulfite complexes. Surface passivation and activation is a slow process in this system, and it is possible that during the reverse positive scan passive layer formation is too slow to follow the 5 mV s^{-1} potential scan rate, and as a result, hysteresis is observed in Figs. 2 and 3.

Both temperature and solution stirring significantly increase the gold deposition rate when polarization is more negative than −0.55 V. This potential value corresponds to the limiting current density. Since for practical purposes the plating current density should be below the limiting value, increasing temperature has no practical advantage for gold plating from sulfite solution.

The electrochemical reduction kinetics of gold were investigated by means of EIS. In a preliminary study we used a simple model, consisting of polarization resistor and parallel capacitor (capacitor and resistor connected in parallel). The latter roughly corresponds to charge transfer resistance (R_{ct}) and double layer capacitance (C_D). The lower the alternating current frequency, the more visible are changes of capacitance and resistance. We have chosen a frequency of 3 Hz (Fig. 4). Otherwise, lower frequencies are used; a lower potential scan rate can be applied. This question we solved experimentally: performing measurements at the potential scan rate from 0.2 mV s^{-1} to higher values. Experimental deviations started when the potential scan rate was above 4–5 mV s^{-1}. So we choose the 2 mV s^{-1} rate.

Classical electrochemical theory [24] predicts that maximal R_{ct} values should be obtained near the equilibrium potential, and with increasing polarization R_{ct} it should decrease exponentially. In our system we observe classical behavior only for a small polarization (up to −0.05 V) and for a large polarization (from −0.3 V) (see Fig. 4, curves 1 and 2).

In the range in between, the opposite trend is observed, and the R_{ct} rapidly increases with polarization. This effect is possible only when the active electrode area decreases during the negative potential scan as a result of surface passivation. Moreover, the active surface area decreases more rapidly than R_{ct} increases. Double layer capacitance as a function of electrode potential is shown in Fig. 4. Curves 3 and 4 suggest that the surface is blocked by a dielectric layer and not by chemically adsorbed ions, since in the latter case the double layer capacitance would increase with potential. The maximal surface coverage should coincide with the C_D minimum observed at −0.45 V. Since the C_D minimum and R_{ct} maximum do not coincide, we conclude that the active surface area slowly decreases near the maximal coverage. In Fig. 4 we show that the potential scan rate significantly affects the impedance parameters, which suggests that activation and passivation rates in this system are rather slow. Similar effects were observed in a previous study [17].

3.2 Sulfite adsorption on the gold electrode surface

It was mentioned above that extremely high polarization of electroreduction of gold sulfite complexes appears probably due to electrode surface passivation caused by slow

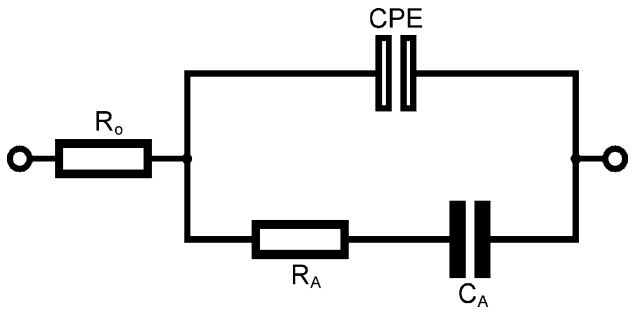

Fig. 5 Equivalent circuit for sulfite adsorption on gold. R_0—uncompensated solution resistance, CPE—constant phase element, R_A and C_A—adsorption resistance and capacitance, respectively

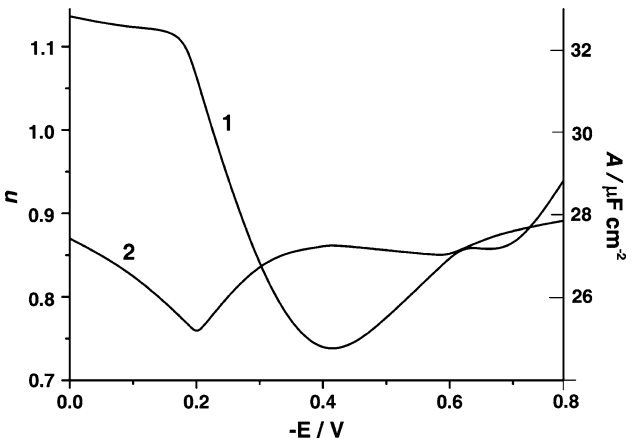

Fig. 6 CPE argument A (curve 1) and exponential number n (curve 2) plots versus Au electrode potential in 0.5 M Na_2SO_3 solution

chemisorption of sulfite ions. We studied sulfite adsorption on gold electrodes separately by means of EIS and EQCM. Impedance spectra were acquired in the frequency range 0.05–4,000 Hz. Spectral analysis immediately revealed that experimental results cannot be fitted to the classical equivalent circuit, and that the double layer capacitor should be replaced by a constant phase element (CPE) (Fig. 5).

Analyzing EIS data, according to a given equivalent circuit (Fig. 5) it would be necessary to connect the charge transfer resistance in parallel to CPE. Connected resistance could represent the processes of oxidation–reduction or the adsorption–desorption of solution impurities. However, analysis of experimental data showed that the impact of R_{ct} is negligible. So we omitted this resistance in order to decrease the number of elements in the suggested equivalent circuit.

A values of CPE (Fig. 6) are within the 24.5 and 33 μF cm^{-2} limits with a flat minimum at −0.42 V. Taking into account other studies [18] the minimum may be caused by the transition of chemically adsorbed sulfite layer into dielectric film (for example, sulfur). Since A minimum potential coincides with the C_D minimum potential (compare Figs. 4 and 6) observed for the gold sulfite complex reduction, we conclude that the passive layer consists of sulfite ions. The electrochemical crystallization effects of gold (Fig. 4) explain the difference in the absolute capacitance values. Changes in n show that the greatest expected deviation from the ideal capacitor is observed at −0.2 V (Fig. 6), where, presumably, the transition of adsorbed sulfite into a dielectric layer is initiating and the surface reaches the highest level of inhomogeneity. At more negative potentials CPE behaves more like a simple capacitor.

Adsorption capacitance (C_A) and resistance (R_A) as a function of electrode potential is shown in the Fig. 7. The change in electrode surface coverage takes place more rapidly near −0.2 V (here C_A is equal to 11 μF cm^{-2}), precisely where the Au surface is inhomogeneous (Fig. 6, curve 2). As can be seen from Fig. 7 adsorption capacitance achieves minimal values at −0.8 V i.e. in the potential range where the Au surface is not covered by a passive layer and the reduction of gold sulfite complexes is limited only by diffusion (see Fig. 2). It is worth noting that the adsorption rate is minimal at this potential (R_A = 20 Ω cm^{-2}).

In the EQCM study the electrode potential was scanned from −0.9 V positively in 25 mV increments. The shift of the resonance frequency Δf as a function of electrode potential is shown in Fig. 8. Nearly linear changes with electrode potential were observed from −0.8 V (Δf = 1 Hz) to −0.25 V (Δf = −26 Hz). This frequency change corresponds to the mass increase up to 160 ng. The further potential scan up to 0 V did not affect the resonance frequency, showing that electrode mass did not change with potential. To conclude both EIS and EQCM data show that we can propose that the gold surface is inhomogeneous in the potential region from −0.2 to −0.4 V. The change of exponential number n (Fig. 6, curve 2) and study [18]

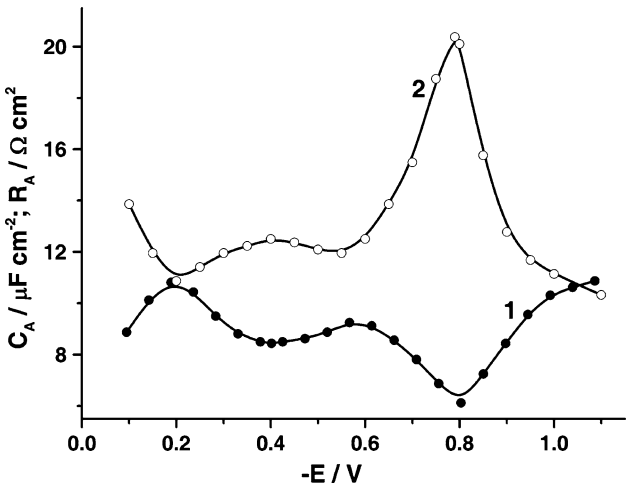

Fig. 7 Adsorption capacitance C_A (curve 1) and resistance R_A (curve 2) plots versus Au electrode potential in 0.5 M Na_2SO_3 solution

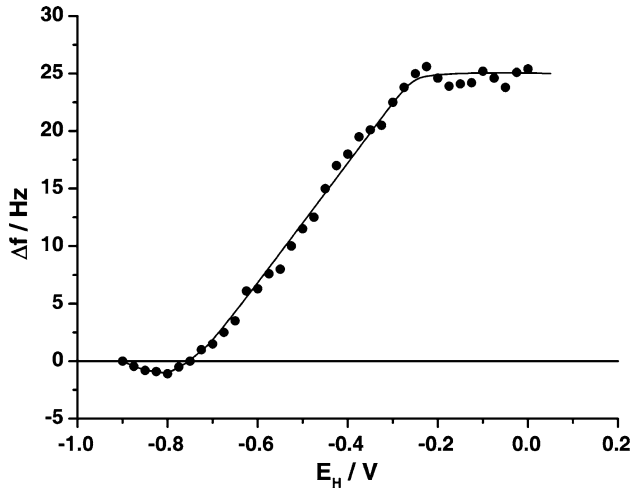

Fig. 8 The shift of the resonance frequency as a function of Au electrode potential in 0.5 M Na_2SO_3 solution

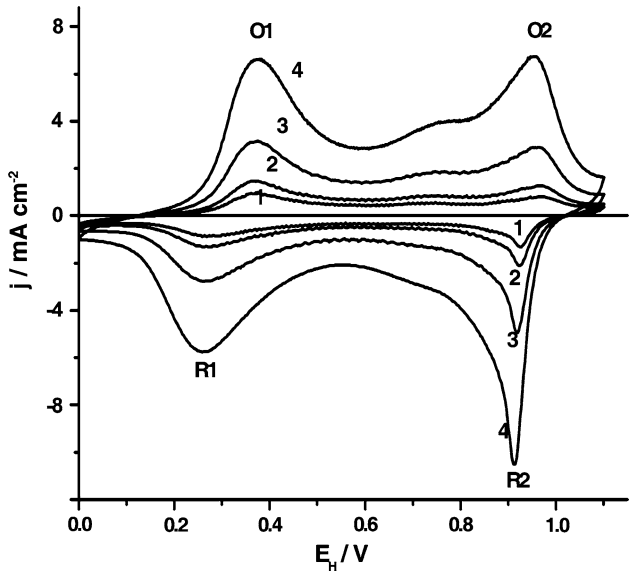

Fig. 9 Cyclic voltammetry curves for polyaniline deposited on gold film in 0.5 M $HClO_4$ solution. Potential scan rate is as follows (V s^{-1}): 1—0.008, 2—0.012, 3—0.025, and 4—0.050

suggested that the surface of gold electrode is pasivated by a dielectric layer (sulfur). In that case sulfur occurs on the surface in the form of a film containing S–S bonds. So the surface coverage Θ was calculated in accordance with parameters of rhombic modification sulfur lattices, where the length of S–S bond is equal to 0.206 nm [25]. Thus a 160 ng amount of sulfur determined by EQCM should cover a 1.05 cm^2 surface. Taking into account the used geometrical area of the working electrode (0.12 cm^2) the surface coverage ($\Theta \approx 5$) was calculated. The obtained value should be less because the roughness of the gold surface was not taken into consideration. In any case it is reliable that $\Theta \geq 1$.

Based on the CPE parameter values and the signal observed in the Raman spectrum [18], typical for S–S bond, we conclude that the gold surface is covered with a dielectric layer, most likely sulfur. Also we can propose that the thickness of the dielectric layer is not bigger than the monoatomic sulfur layer, because the double layer capacitance (Fig. 6, factor *A*) decreases slowly enough.

3.3 Gold film as a substrate for electrochemical polymerization

Electrochemical aniline polymerization on base metals is complicated; making the production of cheap sensors, and particularly biosensors, problematical. We tested the possibility of using the gold sublayer as a possible substrate. Aniline polymerization was studied on the 1 μm thick Au film deposited on a titanium substrate from the sulfite electrolyte. Aniline was polymerized by electrode potential cycling between 0.0 and 1.05 V in a solution with 0.2 M of aniline and 0.5 M of $HClO_4$. The appearance of cathodic and anodic current peaks shows polymer layer formation. After 30–40 potential cycles a sufficiently thick polyanilline layer was formed on the surface. The electrode was thoroughly washed, and the cyclic voltammograms were recorded in the 0.5 M $HClO_4$ solution. In Fig. 9 we show the typical curves obtained at various scan rates. They exhibit two oxidation (O1 and O2) and two reduction (R1 and R2) current peaks, thus confirming published data in which it is stated that the oxidation and reduction of polyaniline happens in two steps. The curves obtained are identical to those obtained for a bulk gold electrode [26]. Regardless of the number of potential scans and the contact time with solution, voltammetric curves were ideally reproducible. We conclude that even a thin gold layer deposited on titanium can be used for the formation of a polyaniline layer suitable for the composition of a wide range of sensors.

In Fig. 10 the peak current as a function of potential scan rate is shown. The currents of all four peaks linearly increase with the scan rate, suggesting that the processes of oxidation and reduction are not limited by diffusion and proceed according to adsorption mechanism.

EIS was used for further characterization of the polyaniline layer. The impedance spectra were determined by varying electrode potential from −0.2 to 0.9 V in 0.05–0.1 V increments, and back from 0.9 to −0.2 V. Both literature data and the cyclic voltammograms (Fig. 9) showed that the oxidation–reduction process of polyaniline proceeds in two stages. If the following stages proceed in rather different potential regions, it would be enough to use only a single RC element in modeling the equivalent circuit. However, good convergence between the experimental EIS data and the model was obtained only when two separate

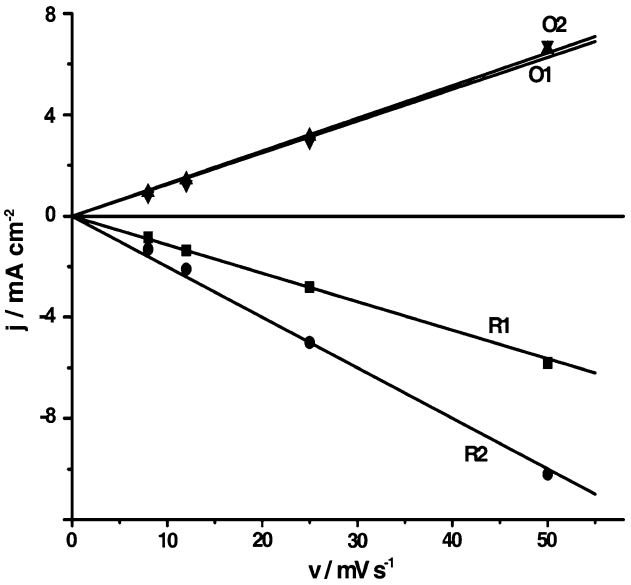

Fig. 10 Anodic (O1 and O2) and cathodic (R1 and R2) current maxima plots versus potential scan rate

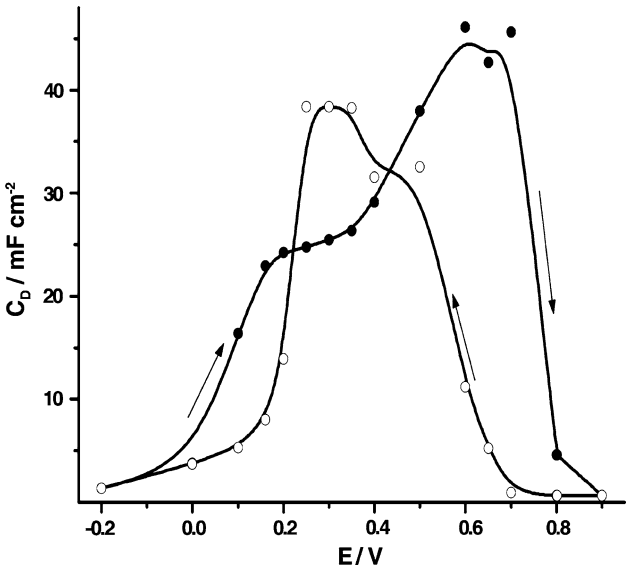

Fig. 12 Double layer capacitance as a function of Au/polyaniline electrode potential. Arrows show the potential scan direction

elements of R_1C_1 and R_2C_2 were included into the equivalent circuit. In our opinion, the diffusion of counterions is negligible in the investigated frequency range and no circuit elements related with diffusion are necessary. Thus our suggested modeling equivalent circuit consists of CPE and two parallel adsorption circuits (Fig. 11). CPE represents the double layer capacity of an inhomogeneous substrate, and the two adsorption circuits correspond to the first and second polyaniline oxidation–reduction reactions respectively. The quality of fit was better than 2−3% in the entire frequency range studied from 0.05 to 4,000 Hz (data not shown). The equivalent circuit analysis shows that the charging of the double layer capacity C_D dominates at higher frequencies and only for frequencies below 3 Hz

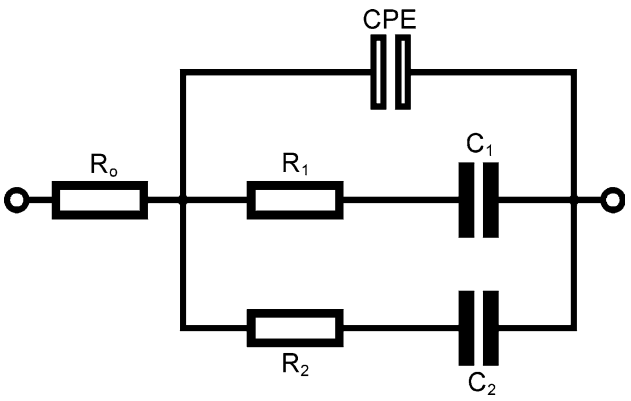

Fig. 11 Equivalent circuit for polyaniline adsorption and desorption on the gold film electrode. R_0 is the uncompensated solution resistance, CPE is the constant phase element, R_1C_1 and R_2C_2 are adsorption resistance and capacitance of the first and the second step, respectively

does the polyaniline oxidation and reduction (R_1C_1 and R_2C_2) become predominant. Maxima of the adsorption capacity C_1 and C_2, (values of which reach up to 200 mF cm^{-2},) coincide with the current maxima observed in voltammetric curves (Fig. 9).

Extremely high double layer capacitance (up to 40–50 mF cm^{-2} at 0.6 V during the positive scan, and at 0.2 V during negative scan) shows that the real surface area of a polyaniline layer is very large. These potential values (0.6 and 0.2 V) are within the two polyaniline oxidation and reduction steps in voltammetric curves (Fig. 9), where the polyaniline layer exhibits high conductivity. Outside this potential range the capacitance values are rather small and drop to near zero at −0.2 and 0.9 V. Completely reduced or oxidized polyaniline shows insulating layer properties. The C_D meaning is obvious only in the conducting region (from 0.15 to 0.7 V), where CPE n values are above or equal to 0.8 (Fig. 12). Outside this potential window n values decrease and the meaning of C_D is not clear.

4 Conclusions

The standard electrochemical reduction potential of gold(I) sulfite complex reduction is equal to 0.116 V. Upon solution stirring and temperature increase the rate of electrochemical reduction increases, albeit only for electrode potentials below −0.55 V. Neither solution stirring nor temperature increase are of commercial interest in gold plating. The electroreduction of gold from sulfite solutions proceeds through passive layer formation at potentials above

−0.55 V. The passive layer consists of chemically adsorbed sulfite ions and sulfur. High-quality gold films were obtained from sulfite solutions. These films can be used for conducting polymer synthesis with possible application in sensor technology.

Acknowledgments The authors thank the Lithuanian State Science and Studies Foundation (grant No. B-34/2008) for partial financial support.

References

1. Brahim S, Wilson AM, Narinesingh D et al (2003) Microchim Acta 143:123
2. Sadik OA, Ngundi M, Wanekaya A (2003) Microchim Acta 143:187
3. Tarasevich MR (1990) The electrochemistry of polymers. Nauka, Moscow
4. Kaiser H (2002) Edelmetallschichten. Leutze Verlag, Bad Saulgau
5. Smith PT (1962) US patent No. 3.059.789
6. Morrissey RJ (1993) Plat Surf Finish 80:75
7. Dauksher WJ, Resnick DJ, Yanof AW (1994) Microelectron Eng 23:235
8. Ehrfeld W, Lehr H (1995) Radiat Phys Chem 45:349
9. Okinaka J, Hoshino M (1998) Gold Bull 31:3
10. Green TA, Liew MJ, Roy S (2003) J Electrochem Soc 150:C104
11. Pechewitskij BJ, Erenburg AM (1970) Izv Sib Otdel AN SSSR Ser Khim Nauk 4:24
12. Wilkinson P (1986) Gold Bull 19:75
13. Shirai N, Yoshimura S, Sato E (1989) J Surf Finish Soc Jpn 40:543
14. Honma H, Hagiwara K (1995) J Electrochem Soc 142:81
15. Honma H, Kagaya Y (1993) J Electrochem Soc 140:L135
16. Baltrūnas G, Valiūnienė A, Valiūnas R (2003) Pol J Chem 77:1819
17. Varga K, Baradlai P, Vertes A (1997) Electrochim Acta 42:1143
18. Fanigliulo A, Bozzini B (2002) Trans Inst Met Finish 80:132
19. Osaka T, Kato N, Sato J et al (2001) J Electrochem Soc 48:C659
20. Stoynov ZB, Grafov BM, Savova-Stoinov BS et al (1991) Electrochemical impedance. Nauka, Moscow
21. Kupper M, Baltrūnas G, Lowe H (1997) Galvanotechnik 88:2906
22. Baltrūnas G, Drunga V, Švedas D (1994) J Electroanal Chem 365:67
23. Vetter KJ (1967) Electrochemical kinetics. Academic Press, New York
24. Grafov BM, Ukshe EA (1973) The electrochemical AC circuits. Nauka, Moscow
25. Wells AF (1986) Structural inorganic chemistry. Clarendon Press, Oxford
26. Guiseppielie A, Pradhan SR, Wilson AM et al (1993) Chem Mater 5:1474